Observation of Nonclassical Correlations in Biphotons Generated from an Ensemble of Pure Two-Level Atoms

Michelle O. Araújo, Lucas S. Marinho, and Daniel Felinto
Departamento de Física, Universidade Federal de Pernambuco, 50670-901 Recife, Pernambuco, Brazil

(Received 31 July 2021; revised 15 January 2022; accepted 24 January 2022; published 22 February 2022)

We report the experimental verification of nonclassical correlations for an unfiltered spontaneous four-wave mixing process in an ensemble of cold two-level atoms, confirming theoretical predictions by Du *et al.* in 2007 for the violation of a Cauchy-Schwarz inequality in the system, and obtaining $R = (1.98 \pm 0.03) \not\leq 1$. Quantum correlations are observed in a nanoseconds timescale in the interference between the central exciting frequency and sidebands dislocated by the detuning to the atomic resonance. They prevail over the noise background coming from Rayleigh scattering from the same optical transition. These correlations are fragile with respect to processes that disturb the phase of the atomic excitation, but are robust to variations in number of atoms and to increasing light intensities.

DOI: 10.1103/PhysRevLett.128.083601

Four-wave mixing (FWM) is a nonlinear parametric process in which a fourth optical field is generated in a medium as a result of the action of three other fields [1]. Commonly, two pump beams are employed to enhance a weak probe beam simultaneously with the generation of the FWM signal. In atomic systems, FWM has been an important source of squeezing and nonclassical correlations for light fields (probe and signal) for more than three decades [2–8]. Since 2001, with the introduction of the Duan-Lukin-Cirac-Zoller protocol for long distance quantum communication [9], quantum correlations from spontaneous four-wave mixing (SFWM) have been recognized as a critical resource for quantum information applications. In SFWM, spontaneous emission in a particular direction plays the role of the weak probe field. Several groups in the last 15 years have demonstrated the capability of SFWM to generate highly correlated photon pairs [10–17], and even applied it to implement crucial portions of the Duan-Lukin-Cirac-Zoller protocol [18,19].

In order to observe quantum correlations in SFWM, various techniques have been employed to filter the correlated photons from the large backgrounds coming from elastic Rayleigh scattering of the pump beams. Rayleigh scattering is a ubiquitous process in which small particles scatter light with frequencies close to that of the excitation field [20]. For any particular transition between two levels in an ensemble of atoms, this process results in scattered light with photon statistics of a thermal light source [21,22]. To eliminate this contribution, SFWM experiments typically employ a more complex level structure for the atoms, generating light with polarizations or frequencies significantly different from the pump beams.

In 2007, however, Du *et al.* pointed out theoretically that quantum correlations in SFWM from an ensemble of two-level atoms should overcome the Rayleigh scattering background, revealing its nonclassical nature even without the use of any filter [23–25]. This result was surprising for a number of reasons. First, a nonclassical signal was surpassing a central process for classical optics under relatively mundane conditions. Second, it is generally assumed that quantum correlations in SFWM in free space have a better chance of prevailing at high numbers of atoms and low pump intensities since these factors would enhance, respectively, the parametric process behind FWM [26,27] and the purity of the quantum states [9,13]. However, the nonclassical correlations predicted by Du *et al.* were largely insensitive to both pump intensity and number of atoms in the ensemble, indicating its robustness for a large range of parameters. Third, the theory in Refs. [23,24] was deduced in a limit particularly suitable to classical models [28], serving as first approximation for a large number of systems, which highlights the necessity of quantum theory to explain the whole body of phenomena for any range of parameters.

Unfortunately, the overall message of the works by Du *et al.* was significantly undermined by the lack of experimental demonstration of these nonclassical correlations on the accompanying experiments [23,24]. In the present work, we finally close this gap and report a series of experiments confirming the core claims of the theory in Refs. [23,24]. We observe not only the nonclassical correlations without any filter for the Rayleigh scattering background, but also its insensitivity with variations in pump power and number of atoms. This opens numerous possibilities. First, if the correlations were strong enough to be observed without filters, we expect to enhance them significantly, in the future, by filtering the light component at the pump frequency. Second, multipartite quantum

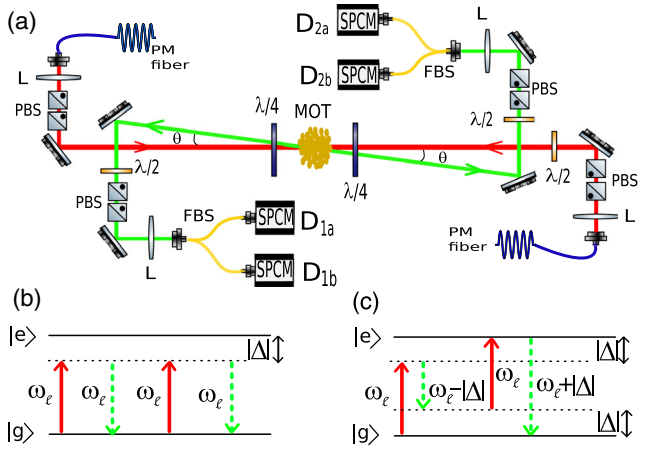

FIG. 1. (a) Experimental setup for spontaneous four-wave mixing (SFWM) from a cold ensemble of pure two-level atoms. (b) and (c) show the two possible pathways for SFWM. MOT, magneto-optical trap; PBS, polarizing beam splitter; SPCM, single-photon counting model; FBS, fiber beam splitter; L, lens; $\lambda/2$ ($\lambda/4$), half-wave (quarter-wave) plate; PM fiber, polarization-maintaining fiber.

correlations should play an important role in this system, since their symmetry allows for SFWM in two other directions [29,30] not explored here or in the previous theoretical works. Finally, the independence of the effect with pump power and number of atoms may favor future applications since it allows for more amenable conditions of moderate optical depths and higher rates of biphoton generation.

The experimental scheme under consideration is shown in Fig. 1(a), with two counterpropagating pump fields (in red) spontaneously generating pairs of photons (fields 1 and 2, in green) emitted in opposite directions, forming an angle θ with the pump fields. This backward SFWM process occurs mainly through two different pathways: either the emitted photons have frequencies $\omega_1 = \omega_2 = \omega_l$ [Fig. 1(b)], with ω_l the excitation-laser frequency, or they have frequencies $\omega_1, \omega_2 = \omega_l \pm \Delta$ [Fig. 1(c)], with $\Delta = \omega_l - \omega_a$ and ω_a the atomic resonance frequency. These different contributions interfere in the observation of fields 1 and 2, resulting in a beating in the intensity cross-correlation function $g_{12}(t, t+\tau) = \langle I_{D1}(t) I_{D2}(t+\tau)\rangle / \langle I_{D1}(t)\rangle \langle I_{D2}(t+\tau)\rangle$, with $I_{Di}(t)$ the intensity of light at time t measured at a detector for field i ($i = 1, 2$), and $\langle \cdots \rangle$ denoting an ensemble average over many samples. Assuming an ergodic system and in the simple limit of large detunings, short delays, and low excitation power, the theoretical analysis of Refs. [23] and [24] leads to

$$g_{12}(\tau) = 1 + \frac{4}{\pi^2}[1 + e^{-\Gamma|\tau|} - 2\cos(\Delta|\tau|)e^{-\Gamma|\tau|/2}], \quad (1)$$

with Γ the natural decay rate of the excited state. The maximum value of this quantity is $g_{12}^{\max} \approx 2.62$. The fact that $g_{12}^{\max} > 2$ for the cross-correlation function is quite significant for photon pair generation by SFWM. The corresponding autocorrelation functions are expected to be $g_{11}, g_{22} \approx 2$ due to the field's thermal statistics. The simplest measure of quantum correlation for biphoton generation in SFWM is the observation of $g_{12} > g_{11}, g_{22}$ [10–15,17] since this condition results in the violation of a Cauchy-Schwarz inequality valid for all classical fields [31]. This observation essentially contradicts any theory for which the probability of photodetection is proportional to the classical intensity of light.

As anticipated above, Eq. (1) does not depend on pump power or the number of atoms, since the product of independent Rayleigh scatterings in fields 1 and 2 depends on these quantities in a similar way as the FWM process itself [24], rendering normalized quantities such as g_{12} insensitive to these parameters. The Rayleigh scattering is an elastic process, with the scattered photon having the same energy as a pump photon. However, it is not phase matched, since the change in direction of the photon implies a change of linear momentum of the small scatterer. SFWM, on the other hand, is a phase-matching process, with both momentum and energy conservation among the light fields. In the situation considered here, thus, the phase-matching condition enhances the efficiency of the process enough to surpass the product of two independent Rayleigh scatters.

Our ensemble is a cold cloud of Rb^{87} atoms obtained from a magneto-optical trap. The trap laser and magnetic field are turned off 1 ms prior to turning on the pump fields, but the repumper laser is kept on for an extra 900 μs to allow for the preparation of all atoms in the $5S_{1/2}$ ($F = 2$) hyperfine ground state [22]. 50 μs after turning off the repumper laser, counterpropagating pump fields of same intensity I_p are turned on for 1 ms. After that, the trap is turned on again and the cycle is repeated at a 40 Hz rate. As shown in Fig. 1(a), the pump fields have their linear polarizations transformed to the same circular σ^+ polarization by quarter-wave ($\lambda/4$) plates on each side of the atomic ensemble, resulting in optical pumping to the $5S_{1/2}$ ($F = 2, m_F = 2$) Zeeman sublevel [32,33]. We collect fields 1 and 2 using single mode fiber, with $\theta = 3°$. Prior to the fibers, the $\lambda/4$ plates transform the circular polarization of the emitted photons back to linear polarization. The photon's degree of polarization is verified to be $(99.0 \pm 0.2)\%$. The 4σ beam diameters at the ensemble are 420 μm and 140 μm for pump fields and detection modes, respectively. The optical depth is $OD \approx 15$, corresponding to $N \approx 10^6$ atoms contributing to light in the detected modes [17,27]. Δ is the detuning from the excited state $5P_{3/2}$ ($F = 3$). The two emitted fields go through fiber beam splitters toward two separate avalanche photodetectors for fields 1 (D_{1a}, D_{1b}) and 2 (D_{2a}, D_{2b}), respectively. The detectors are single-photon counting modules (model SPCM-AQRH-13-FC from Perkin Elmer) with outputs directed to a multiple-event time digitizer with 100 ps time resolution (model MCS6A from FAST ComTec).

The relatively small nonclassical correlations coming from Eq. (1), when compared to the state of the art of SFWM [13], imply that these are more fragile, easier to lose. For this reason, the first attempts to measure these nonclassical correlations were not successful [23,24]. The experimental observation of nonclassical correlations reported here was possible due to various improvements with respect to the apparatus and methods of Refs. [23,24]. The first was to optically pump the atoms toward a single Zeeman sublevel, resulting in a pure two-level system, since atoms in different Zeeman sublevels participate in different parametric processes and do not constructively interfere with each other to enhance the SFWM [26]. The second improvement was to turn off the magnetic field and repumper laser during trials, since they could scramble the collective phase throughout the atomic ensemble. Particularly, turning off the repumper laser implies that our system is no longer ergodic, since we observe now a clear temporal dynamics related to optical pumping. Thus, the methodology to measure the effect behind Eq. (1) had to change, focusing in ensemble averages rather than time averages. Finally, the time resolution of the coincidence electronics was improved by a factor of 10, allowing us to probe faster oscillations for larger detunings.

As just mentioned, during each 1 ms trial period, the detection probabilities vary due to spurious optical pumping to the $5S_{1/2}$ ($F = 1$) level, coming from the action of a residual magnetic field of about 23 mG that weakly couples the atoms to noncycling transitions [22,33]. This is shown in Fig. 2(a), where we plot two of the four single detection probabilities, namely, $p^T_{1a}(t)$ and $p^T_{2b}(t)$ for detectors D_{1a} and D_{2b}, respectively. These probabilities were first obtained as ensemble averages for each time t over all trial periods, and later averaged over a time interval of $T = 10\ \mu$s around t. Considering that Rayleigh scattering would result in $p^T_{1a}, p^T_{2b} \propto N$, we observe then an initial period of optical pump in the Zeeman structure, as atoms accumulate in the $m_F = +2$ sublevel. Later, the spurious optical pump to the hyperfine $F = 1$ level slowly decreases the overall population in $F = 2$. For Fig. 2, $I_p = 126\ \mathrm{mW/cm^2}$ (measured power per area) and $\Delta = +20\ \Gamma$.

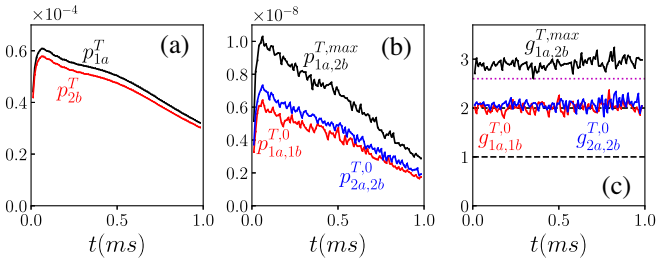

FIG. 2. (a) Probabilities for single detections and (b) maximum joint detections as a function of time, with averages over $T = 10\ \mu$s. (c) Normalized second order correlation functions for the joint probabilities in (b). The dashed lines indicate the levels of 1 for no correlation, 2 for thermal correlations, and 2.62 for the maximum of Eq. (1).

Figure 2(b) plots three of the joint probabilities p^T_{ij}, between detectors i and j, characterizing the biphoton correlations. For each of them, we plotted their maxima with respect to variations of τ for a particular instant t, given by $p^{T,\max}_{i,j}$. In the case of joint detections for the same field, their maxima occur at $\tau = 0$, represented by $p^{T,0}_{1a,1b}(t)$ and $p^{T,0}_{2a,2b}(t)$, respectively. As expected, joint probabilities are more sensitive to the number of atoms than single probabilities, since even uncorrelated detections would give $p^T_i p^T_j \propto N^2$. Most importantly, however, is that $p^{T,\max}_{1a,2b}(t)$ is always larger than $p^{T,0}_{1a,1b}(t)$ and $p^{T,0}_{2a,2b}(t)$, indicating already the presence of nonclassical correlations. As previously discussed, these correlations are better quantified through the corresponding normalized functions $g^{T,\max}_{ij}(t)$ of Fig. 2(c). We observe then $g^{T,0}_{1a,1b}(t) \approx g^{T,0}_{2a,2b}(t) \approx 2$, as expected for fields with thermal statistics [22,34]. On the other hand, we have always $g^{T,\max}_{1a,2b}(t) > 2$.

As predicted from Eq. (1), $g^{T,\max}_{1a,2b}(t)$ is almost independent of the number of atoms. We observe this trend for all correlation functions and for every τ. In this way, we can capture well the behavior of the system by averaging the correlation functions during the whole 1 ms trial period, defining $\bar{g}_{ij}(\tau) = g^{T=1\ \mathrm{ms}}_{ij}(0.5\ \mathrm{ms}, 0.5\ \mathrm{ms} + \tau)$. The results of Fig. 2 were acquired with enough statistics to determine any correlation function or the violation of the Cauchy-Schwarz inequality throughout the whole 1 ms trial period. On the other hand, the averaged $\bar{g}_{ij}(\tau)$ allows for a broader variation of parameters in the system, without the need to accumulate as much data. We can then define the corresponding averaged Cauchy-Schwarz inequality for classical fields as [31]

$$R(\tau) = \frac{\bar{g}_{1a,2b}(\tau)\bar{g}_{1b,2a}(\tau)}{\bar{g}_{1a,1b}(0)\bar{g}_{2a,2b}(0)} \leq 1. \tag{2}$$

Figure 3(a), then, plots all correlation functions required to measure $R(\tau)$ for the parameters of Fig. 2 and up to $|\tau| = 30$ ns. We observe the same oscillatory behavior for the functions $g_{12}(\tau)$ as predicted in Eq. (1). The dashed lines provide the same reference values of Fig. 2(c), and the experimental values of $\bar{g}_{12}(\tau)$ clearly exceed the maximum prediction for Eq. (1). The results for the violation of the Cauchy-Schwarz inequality are shown in Fig. 3(b) for two different pairs of detuning and pump intensity: ($+20\Gamma$, $126\ \mathrm{mW/cm^2}$) and ($+40\Gamma$, $250\ \mathrm{mW/cm^2}$). For $\Delta = +20\Gamma$, we observed a maximum $R_{\max} = (1.98 \pm 0.03) \not\leq 1$, a violation by 33 standard deviations. The dashed lines again provide some reference values: $R = 0.25$ for no cross-correlation, $R = 1$ for the maximum classical correlations, and $R = 1.71$ for the maximum value predicted by Eq. (1). Again, violations larger than predicted by Eq. (1) are observed.

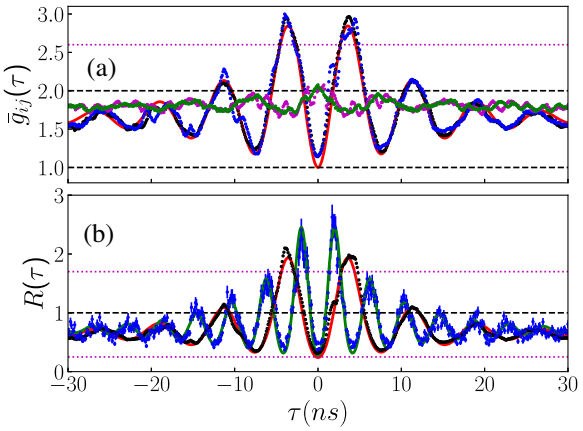

FIG. 3. (a) Circles provide measurements of the second order correlation functions, as a function of τ, between detectors $1a$ and $2b$ (black), $1b$ and $2a$ (blue), $1a$ and $1b$ (magenta), $2a$ and $2b$ (green). Parameters and dashed lines are the same as for Fig. 2. Red solid line provides a fit to Eq. (3). (b) Circles provide measurements of R for $\Delta = +20\Gamma$ and $I_p = 126$ mW/cm^2 (black) and $\Delta = +40\ \Gamma$ and $I_p = 250$ mW/cm^2 (blue). Values above one indicate violation of a Cauchy-Schwarz inequality for classical fields. Dotted lines provide maximum and minimum values of Eq. (1), while solid lines are fits to Eq. (3).

For a better comparison with the experimental data, we had to empirically modify Eq. (1) to

$$g_{12}^{e}(\tau) = 1 + \frac{4f}{\pi^2}[1 + e^{-\chi\Gamma|\tau|} - 2\cos(\Delta'|\tau|)e^{-\chi\Gamma|\tau|/2}], \quad (3)$$

with f, χ, and Δ' as fitting parameters. The solid line in Fig. 3(a) provides the fit to Eq. (3), resulting in $\Delta' = (21.53 \pm 0.07)\ \Gamma$, $f = 1.58 \pm 0.01$, and $\chi = 5.1 \pm 0.1$. The value $\Delta' \approx \Delta$ is consistent with Eq. (1). The value $f > 1$, on the other hand, indicates stronger correlations. The most striking difference, however, is the enhanced natural decay represented by the value of $\chi > 1$, which may indicate the occurrence of collective enhancement in the system, as observed in other experiments under similar conditions [17,35]. Such collective enhancement may also be related to the observation of $f > 1$, since it also affects the directionality of the emitted photons [27]. Using the experimental values for the autocorrelation function at $\tau = 0$ and Eq. (2), the solid line in Fig. 3(a) results in the red solid line in Fig. 3(b). A similar procedure is used for the green solid line for the $\Delta = +40\ \Gamma$ data. In this case, we obtain $\Delta' = (39.5 \pm 0.1)\ \Gamma$, $f = 1.53 \pm 0.03$, and $\chi = 5.6 \pm 0.3$.

$R_{\max}$ values measured by this procedure for various parameters are plotted in Fig. 4. The filled black circles were obtained by changing the detuning with a fixed pump intensity of $I_p = 250$ mW/cm^2. For this experimental sequence, the largest scattering rate is obtained for $\Delta = +20\ \Gamma$, and involved detection rates already close (one tenth) to the saturation rate of our detectors.

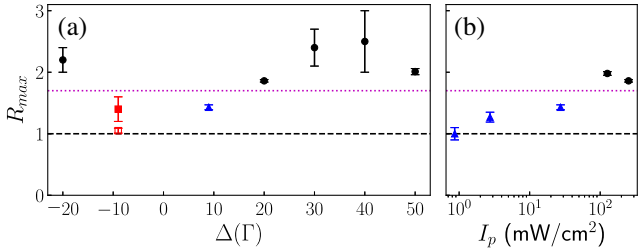

FIG. 4. $R_{\max}$ as a function of (a) detuning and (b) pump intensity. For (a), we have $I_p = 250$ mW/cm^2 (black filled circles), 14 mW/cm^2 (red filled square), and 27 mW/cm^2 (blue filled triangle), respectively. The empty square is measured for the same parameters as the filled one, but with the MOT repumper laser turned on continuously. For (b), the detunings are $\Delta = +9\ \Gamma$ (blue filled triangles) and $+20\ \Gamma$ (black filled circles). Horizontal lines are the same as for Fig. 3(b).

For smaller detunings, we had then to decrease the intensity of the excitation fields. For $\Delta = +9$ and -9Γ in Fig. 4(a), we used $I_p = 27$ and 14 mW/cm^2, respectively. The $R_{\max}$ values for $\Delta = \pm 9\ \Gamma$ are given by the filled triangle and square, respectively, and represent our optimized values for these detunings. The open square gives the result for the same conditions as the filled square, but with the repumper laser turned on continuously. We observe, then, that the repumper laser substantially decreases the observed correlation, leaving it at the border of the classical region. Figure 4(b) plots some data changing the intensity for two different detunings ($\Delta = +9\Gamma$ and $+20\ \Gamma$) representing quite different conditions of $R_{\max}$. In general, we observe a robust violation $R_{\max} \nleq 1$ for a broad variation of parameters without large variations of its value. This overall behavior is in agreement with Eq. (1), even though the specific shape of the curves and maximum correlations was best approximated by the empirical Eq. (3). In practice, we found $R_{\max}$ mostly affected by alignment of the four-wave mixing fields, polarization optimization, and elimination of other background fields, like the MOT repumper laser. Degradation on these general conditions would set $R_{\max} \leq 1$. However, once the conditions are set for the correlations to rise above the classical limit, they become quite insensitive and robust to large variations of key parameters.

In conclusion, we demonstrated experimentally the nonclassical correlation between photon pairs emitted through SFWM in an ensemble of pure two-level atoms, confirming previous theoretical predictions [23,24]. We also demonstrated the broad independence of the correlation to various experimental parameters that commonly control the purity of photon pairs generated from atomic ensembles, like the number of atoms in the sample and the detection rates (determined by detuning and excitation intensity). We were able to observe clear nonclassical correlations up to detection rates close to the saturation

of our photodetectors. The experimental data, however, also reveal discrepancies with the theoretical predictions, showing larger nonclassical correlations and faster decays, which are currently under investigation. These observations point to the possibility of observing and exploring nonclassical correlations in more mundane situations, over strong backgrounds of uncorrelated photons, stressing the importance of developing complete quantum treatments for situations commonly believed to be well covered by semiclassical theories. Finally, the reported nonclassical correlation may be considerably enhanced by filtering the component of Rayleigh scattering and exploring multipartite correlations to other directions.

This work was supported by the Brazilian funding agencies CNPq (Conselho Nacional de Desenvolvimento Científico e Tecnológico), CAPES (Coordenação de Aperfeićoamento de Pessoal de Nível Superior), and FACEPE (Fundação de Amparo à Ciência e Tecnologia do Estado de Pernambuco) through the programs Programa de Apoio a Núcleos Emergentes and INCT-IQ (Instituto Nacional de Ciência e Tecnologia de Informação Quântica).

M. O. A. and L. S. M. contributed equally to this work.

[1] A. Yariv, *Quantum Electronics* (John Wiley & Sons, New York, 1989).
[2] R. E. Slusher, L. W. Hollberg, B. Yurke, J. C. Mertz, and J. F. Valley, Observation of Squeezed States Generated by Four-Wave Mixing in an Optical Cavity, Phys. Rev. Lett. **55**, 2409 (1985).
[3] M. W. Maeda, P. Kumar, and J. H. Shapiro, Observation of squeezed noise produced by forward four-wave mixing in sodium vapor, Opt. Lett. **12**, 161 (1987).
[4] M. G. Raizen, L. A. Orozco, M. Xiao, T. L. Boyd, and H. J. Kimble, Squeezed-State Generation by the Normal Modes of a Coupled System, Phys. Rev. Lett. **59**, 198 (1987).
[5] M. Vallet, M. Pinard, and G. Grynberg, Generation of twin photon beams in a ring four- wave mixing oscillator, Europhys. Lett. **11**, 739 (1990).
[6] A. Lambrecht, T. Coudreau, A. M. Steinberg, and E. Giacobino, Squeezing with cold atoms, Europhys. Lett. **36**, 93 (1996).
[7] J. Ries, B. Brezger, and A. I. Lvovsky, Experimental vacuum squeezing in rubidium vapor via self-rotation, Phys. Rev. A **68**, 025801 (2003).
[8] C. F. McCormick, V. Boyer, E. Arimondo, and P. D. Lett, Strong relative intensity squeezing by four-wave mixing in rubidium vapor, Opt. Lett. **32**, 178 (2007).
[9] L.-M. Duan, M. D. Lukin, J. I. Cirac, and P. Zoller, Long-distance quantum communication with atomic ensembles and linear optics, Nature (London) **414**, 413 (2001).
[10] A. Kuzmich, W. P. Bowen, A. D. Boozer, A. Boca, C. W. Chou, L.-M. Duan, and H. J. Kimble, Generation of nonclassical photon pairs for scalable quantum communication with atomic ensembles, Nature (London) **423**, 731 (2003).
[11] V. Balic, D. A. Braje, P. Kolchin, G. Y. Yin, and S. E. Harris, Generation of Paired Photons with Controllable Waveforms, Phys. Rev. Lett. **94**, 183601 (2005).
[12] D. N. Matsukevich, T. Chanelière, M. Bhattacharya, S.-Y. Lan, S. D. Jenkins, T. A. B. Kennedy, and A. Kuzmich, Entanglement of a Photon and a Collective Atomic Excitation, Phys. Rev. Lett. **95**, 040405 (2005).
[13] J. Laurat, H. de Riedmatten, D. Felinto, C.-W. Chou, E. W. Schomburg, and H. J. Kimble, Efficient retrieval of a single excitation stored in an atomic ensemble, Opt. Express **14**, 6912 (2006).
[14] J. K. Thompson, J. Simon, H. Loh, and V. Vuletić, A high-brightness source of narrowband, identical-photon pairs, Science **313**, 74 (2006).
[15] B. Zhao, Y.-A. Chen, X.-H. Bao, T. Strassel, C.-S. Chuu, X.-M. Jin, J. Schmiedmayer, Z.-S. Yuan, S. Chen, and J.-W. Pan, A millisecond quantum memory for scalable quantum networks, Nat. Phys. **5**, 95 (2009).
[16] B. Albrecht, P. Farrera, G. Heinze, M. Cristiani, and H. de Riedmatten, Controlled Rephasing of Single Collective Spin Excitations in a Cold Atomic Quantum Memory, Phys. Rev. Lett. **115**, 160501 (2015).
[17] L. Ortiz-Gutiérrez, L. F. Muñoz-Martínez, D. F. Barros, J. E. O. Morales, R. S. N. Moreira, N. D. Alves, A. F. G. Tieco, P. L. Saldanha, and D. Felinto, Experimental Fock-State Superradiance, Phys. Rev. Lett. **120**, 083603 (2018).
[18] C. W. Chou, H. de Riedmatten, D. Felinto, S. V. Polyakov, S. J. van Enk, and H. J. Kimble, Measurement-induced entanglement for excitation stored in remote atomic ensembles, Nature (London) **438**, 828 (2005).
[19] C. W. Chou, J. Laurat, H. Deng, K. S. Choi, H. de Riedmatten, D. Felinto, and H. J. Kimble, Functional quantum nodes for entanglement distribution over scalable quantum networks, Science **316**, 1316 (2007).
[20] J. W. Strutt, On the light from the sky, its polarization and colour, London, Edinburgh, Dublin Philos. Mag. J. Sci. **41**, 107 (1871).
[21] R. Loudon, *The Quantum Theory of Light* (Oxford University Press, New York, 1983).
[22] R. S. N. Moreira, P. J. Cavalcanti, L. F. Muñoz-Martnez, J. E. O. Morales, P. L. Saldanha, J. W. R. Tabosa, and Daniel Felinto, Nonvolatile atomic memory in the spontaneous scattering of light from cold two-level atoms, Opt. Commun. **495**, 127075 (2021).
[23] S. Du, J. Wen, M. H. Rubin, and G. Y. Yin, Four-Wave Mixing and Biphoton Generation in a Two-Level System, Phys. Rev. Lett. **98**, 053601 (2007).
[24] J. Wen, S. Du, and M. H. Rubin, Biphoton generation in a two-level atomic ensemble, Phys. Rev. A **75**, 033809 (2007).
[25] J. Wen, S. Du, M. H. Rubin, and E. Oh, Two-photon beating experiment using biphotons generated from a two-level system, Phys. Rev. A **78**, 033801 (2008).
[26] D. Felinto, C. W. Chou, H. de Riedmatten, S. V. Polyakov, and H. J. Kimble, Control of decoherence in the generation of photon pairs from atomic ensembles, Phys. Rev. A **72**, 053809 (2005).
[27] R. A. de Oliveira, M. S. Mendes, W. S. Martins, P. L. Saldanha, J. W. R. Tabosa, and D. Felinto, Single-photon

superradiance in cold atoms, Phys. Rev. A **90**, 023848 (2014).

[28] L. Allen and J. H. Eberly, *Optical Resonance and Two-Level Atoms* (Dover Publications, New York, 1987).

[29] J. P. Lopez, A. M. G. de Melo, D. Felinto, and J. W. R. Tabosa, Observation of giant gain and coupled parametric oscillations between four optical channels in cascaded four-wave mixing, Phys. Rev. A **100**, 023839 (2019).

[30] J. C. C. Capella, A. M. G. de Melo, J. P. Lopez, J. W. R. Tabosa, and D. Felinto, Atomic memory based on recoil-induced resonances, arXiv:2112.14800.

[31] J. F. Clauser, Experimental distinction between the quantum and classical field-theoretic predictions for the photoelectric effect, Phys. Rev. D **9**, 853 (1974).

[32] A. J. F. de Almeida, M.-A. Maynard, C. Banerjee, D. Felinto, F. Goldfarb, and J. W. R. Tabosa, Nonvolatile optical memory via recoil-induced resonance in a pure two-level system, Phys. Rev. A **94**, 063834 (2016).

[33] See Supplemental Material at http://link.aps.org/supplemental/10.1103/PhysRevLett.128.083601 for additional details on optical pumping in our system.

[34] A. Eloy, Z. Yao, R. Bachelard, W. Guerin, M. Fouch, and R. Kaiser, Diffusing-wave spectroscopy of cold atoms in ballistic motion, Phys. Rev. A **97**, 013810 (2018).

[35] M. O. Araújo, I. Krešić, R. Kaiser, and W. Guerin, Superradiance in a Large and Dilute Cloud of Cold Atoms in the Linear-Optics Regime, Phys. Rev. Lett. **117**, 073002 (2016).